Kinematic Analysis and Dexterity of a New STPM

WANG ZHONGFEI, JI SHIMING, WAN YUEHUA, SUN JIANHUI, OU CHANGJIN, PAN YAN
The MOE Key Laboratory of Mechanical Manufacture and Automation
Zhe Jiang University of Technology
Zhaohui 6 zone, Hangzhou, Zhe Jiang
CHINA

Abstract: - A new spatial translational parallel manipulator (STPM) with fixed prismatic actuators, called 3-PRP$_A$R STPM is proposed. Firstly, the architecture of the new STPM is described, and the angular velocity of the end-effector is analyzed. Secondly, the kinematic modeling is built, and the inverse and the direct kinematic problems are solved in analytical form. The inverse kinematic problem produces two possible solutions for each limb and the direct kinematic problem has two possible solutions theoretically, but they have only one solution due to the assembling manner of the STPM. Furthermore, the reachable workspace of the STPM is determined in a case. The STPM has the workspace advantage along *z* axis and its reachable workspace is a cuboid approximately. Finally, we derived the Jacobian matrix of the STPM, and the distribution of the dexterity characteristics is investigated on the different section. The results show that the dexterity of the STPM decreases from the *z* axis to the workspace boundary, its maximal dexterity distributes on the *z* axis, and each configuration inside of the workspace is far from the singularity.

Key-Words: - Spatial Translational Parallel Manipulator Kinematics Workspace Jacobian Dexterity

1 Introduction

In recent years, the parallel manipulators (PMs) with limited DoFs attracted researchers' attention. Actually, in most tasks, the PMs with limited DoFs have some advantage in terms of cost, maintain, and operation. Among of the limited DoFs PMs, the spatial translational 3-DOF PMs have potentially wide range of application. This paper focuses on spatial translational parallel manipulators (STPMs), that is, the end-effector of manipulators is provided with pure translational motion with respect to the base. They may be particularly valuable for polishing device and machine tools as alternative to traditional serial positioning systems.

The Delta manipulator [1] is perhaps the most famous and successful example of a limited DoFs PM design. Hervé and Sparacino [2] systematically presented a whole class of new STPMs with 4-DOF limbs (the number of DoFs of a limb is defined as which the limb provides with the end-effector with respect to the base), which can be addressed as the Hervé and Sparacino family. Also, Tsai [3], Frisoli [4], and Carricato [5] systematically studied a class STPMs with 5-DOF limbs, independently. This entire class of STPMs can be grouped under the name of the Tsai/Frisoli/Carricato family. This family of STPMs has been studied in detail in [6,7].

In the literature, several STPMs have been proposed that belong to Hervé and Sparacino family. Some have been presented by Hervé, like the Y-Star and the H-Robots [9]. Some others have been studied by other researchers, like the University of Maryland manipulator [10], the Orthoglide machine tool [11], the 3-RRC [12,13], 2- or 3-RPC mechanisms [13,14], and modified Delta Robot [15].

In this work, a new STPM with three parallel mutually and mounted-base actuated P joints is proposed, which has three PRP$_A$R topology limbs. This STPM is modified from the Y-Star [9]. We replace three coplanar actuated P joints in Y-Star with three non-coplanar and parallel mutually prismatic actuators. Owing to this actuated manner has some advantage, such as a more regular workspace, the workspace advantage along direction of actuator, and a few singular configurations.

It is note that throughout the context, the kind of kinematic joints will be addressed using the following symbols: P for prismatic joint, R for revolute joint, H for helical joint, P$_A$ for planar parallelogram joint, C for cylindrical joint.

2 Analysis of the Angular Velocity of the End-Effector

2.1 Architecture Description

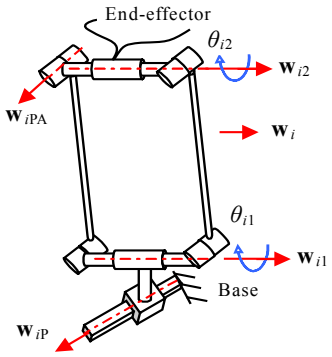

Fig. 1. Sketch of the PRP$_A$R kinematic subchain

The new architecture is comprised of the base and the end-effector by means of three identical limbs, which has PRP$_A$R topology from the base to the end-effector along the each limb. The sketch of a PRP$_A$R kinematic subchain is shown in Fig. 1. It comprises two R joints, one P$_A$ joint, and one P joint. Those joints have some specific geometry conditions: (*a*) the axes of two R joints are parallel to the unit vector $\mathbf{w}_i$, they provide the end-effector with a rotational and a translational motion in a plane which is perpendicular to $\mathbf{w}_i$. (*b*) The P$_A$ joint axis direction $\mathbf{w}_{iPA}$ (which is defined as the direction of axes of the vertex R joints) is perpendicular to the unit vector $\mathbf{w}_i$. (*c*) The P joint is perpendicular to the unit vector $\mathbf{w}_i$. Such a PRP$_A$R kinematic chain output link has 4 DoFs.

The schematic diagram of the 3-PRP$_A$R STPM is shown in Fig. 2. For the entire system, three actuated P joints are parallel mutually, and are mounted on the fixed base. We arrange the unit vector $\mathbf{w}_1$ of first limb and the unit vector $\mathbf{w}_3$ of third limb is parallel mutually, while the unit vector $\mathbf{w}_2$ of second limb is perpendicular to $\mathbf{w}_1$ and $\mathbf{w}_3$.

2.2 Analysis of Angular Velocity

Let the angular velocity of end-effector of STPM in terms of R joints velocities of each limb, as

$$\boldsymbol{\omega} = (\dot{\theta}_{i1} + \dot{\theta}_{i2})\mathbf{w}_i \,,\ i=1,2,3 \qquad (1)$$

where θ_{ij} is the angular variable relative to the *j*-th R joint (*j*=1,2) of the *i*-th limb, and $\mathbf{w}_i$ is a unit vector along the axes of two parallel R joints. We only consider the first limb and second limb, the effect of the third and first limb is uniform, which contributes to the angular velocity of end-effector. Writing (1) for *i*=1,2 respectively, yields

$$\begin{cases} \boldsymbol{\omega} = m_1\mathbf{w}_1 \\ \boldsymbol{\omega} = m_2\mathbf{w}_2 \end{cases} \qquad (2)$$

where $m_1 = \dot{\theta}_{11} + \dot{\theta}_{12}$ and $m_2 = \dot{\theta}_{21} + \dot{\theta}_{22}$. The two vector equations in (2) constitute a linear algebra system of 6 scalar equations with 4 unknown $\dot{\theta}_{ij}$ (*i*=1,2 and *j*=1,2).

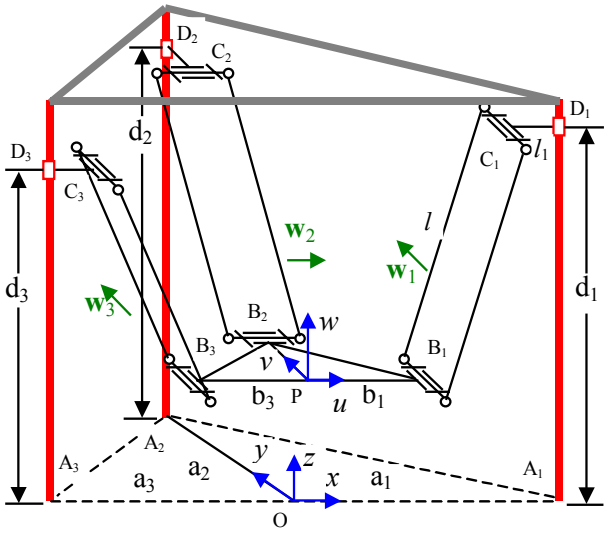

Fig. 1 Schematic diagram of the 3-PRP$_A$R STPM

Taking subtraction for two equations in (2), yields

$$m_1\mathbf{w}_1 - m_2\mathbf{w}_2 = 0 \qquad (3)$$

It can be written (3) in scalar equations form

$$\begin{bmatrix} w_{1x} & -w_{2x} \\ w_{1y} & -w_{2x} \\ w_{1z} & -w_{2x} \end{bmatrix} \begin{bmatrix} m_1 \\ m_2 \end{bmatrix} = 0 \qquad (4)$$

It can be seen that if the former matrix has always full rank, i.e. two limbs of the STPM are satisfied always $\mathbf{w}_1 \neq \mathbf{w}_2$, then only solution of homogeneous system (4) is $m_1=m_2=0$. Therefore, from (1) and (2), it must be

$$\boldsymbol{\omega} = 0\,,\quad \dot{\theta}_{i1} = -\dot{\theta}_{i2} \qquad (5)$$

Obviously, it is conclude that the orientation of the end-effector retains constant with respect to the base at any instant. Thus new architecture reveals pure translational motion, is a STPM. Additionally, such as the STPM doesn't reveal constraint singularity [16], because the orientation of $\mathbf{w}_i$ is invariable throughout the motion of the STPM.

3 The Kinematic Problem

3.1 Kinematic Modeling

The schematic diagram of the 3-PRP$_A$R STPM and the *i*-th limb are shown in Fig. 2 and Fig. 3, respectively. To facilitate the analysis, we assign a fixed Cartesian frame *O* (*x*, *y*, *z*) at the center *O* of A_1A_3 of the base, and a moving frame *P* (*u*, *v*, *w*) at

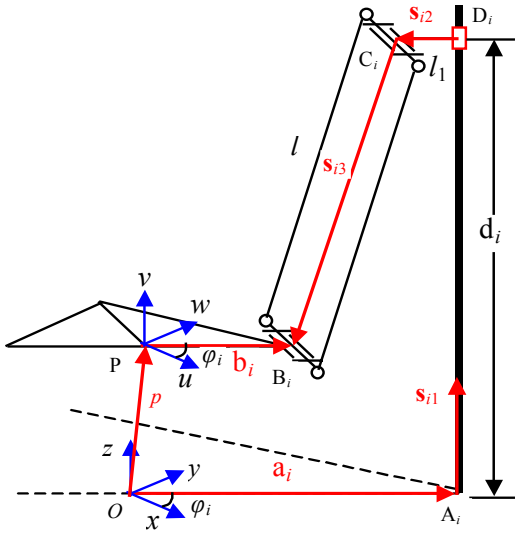

Fig. 3 Schematic representation of the i-th limb

the center P of B_1B_3 on the end-effector, by right-hand rule, with the z and w axes perpendicular to the end-effector, and the x and y axes parallel to the u and v axes, respectively. In addition, the x is along $\mathbf{OA_1}$ direction, the y is along $\mathbf{OA_2}$ direction, the u is along $\mathbf{PB_1}$ direction, and the v is along $\mathbf{PB_2}$ direction. The radius of fixed base and the end-effector satisfied $OA_1= OA_2= OA_3=a$, and $PB_1= PB_2= PB_3=b$.

As shown in Fig. 3, for each limb (i=1,2,3) the following vector-loop equation keeps

$$\mathbf{OP}+\mathbf{PB_i}=\mathbf{OA_i}+\mathbf{A_iD_i}+\mathbf{D_iC_i}+\mathbf{C_iB_i} \qquad (6)$$

where, the orientation of the vector $\mathbf{PB_i}$ remains constant throughout the motion of STPM, because the end-effector has translational motion only. Furthermore, the vector $\mathbf{OA_i}$ and $\mathbf{D_iC_i}$ retains constant with respect to the Cartesian frame O, and the vector $\mathbf{PB_i}$ is constant vector in moving frame P. Therefore, the vector-loop equation can be rewritten for the i-th limb as

$$\mathbf{p}=d_i\mathbf{s}_{i1}+l\mathbf{s}_{i3}+\mathbf{C}_i \qquad (7)$$

where, $\mathbf{C}_i=\mathbf{a}_i-\mathbf{b}_i+l_1\mathbf{s}_{i2}$, the $\mathbf{p}$ is the coordinate of point P in the frame O. The $\mathbf{s}_{i1}$ is a unit vector along P joint, the $\mathbf{d}_i$ is the displacement of the slider. The l_1 is a constant, which is the length of the common normal between the P joint and adjacent R joint axes, and the $\mathbf{s}_{i2}$ is the directional vector, correspondingly. The $\mathbf{s}_{i3}$ is a unit vector along $\mathbf{C_iB_i}$, and its length is l (i.e. the length of P_A joint). Here, these constant vectors are represented as

$$\begin{aligned}&\mathbf{a}_i=[ac_i \quad as_i \quad 0]^T, \mathbf{b}_i=[bc_i \quad bs_i \quad 0]^T,\\ &\mathbf{s}_{i1}=[0 \quad 0 \quad 1]^T, \mathbf{s}_{i2}=[-c_i \quad -s_i \quad 0]^T.\end{aligned} \qquad (8)$$

where, $s_i=sin(\varphi_i)$ and $c_i=cos(\varphi_i)$, the angle φ_i is defined from the x axis to $\mathbf{OA_i}$ in the Cartesian frame O, and also from the u axis to $\mathbf{PB_i}$ in the moving frame P. Apparently, $\varphi_i=(i\text{-}1)(\pi/2)$, for i=1,2,3.

3.2 The Inverse Kinematics

The purpose of the inverse kinematic problem is to solve the actuated variables from a given position of the end-effector.

Rearranging the items of (7) as

$$\mathbf{A}_i-d_i\mathbf{s}_{i1}=l\mathbf{s}_{i3} \qquad (9)$$

where $\mathbf{A}_i=\mathbf{p}-\mathbf{C}_i=\mathbf{p}-(\mathbf{a}_i-\mathbf{b}_i+l_1\mathbf{s}_{i2})$.

Dot-multiplying (9) with itself, eliminating unknown $\mathbf{s}_{i3}$, and rearranging the items, yields

$$d_i^2-2d_i\mathbf{s}_{i1}^T\mathbf{A}_i+\mathbf{A}_i^T\mathbf{A}_i-l^2=0 \qquad (10)$$

Solving (10), the inverse problem is solved

$$d_i=\mathbf{s}_{i1}^T\mathbf{A}_i\pm\sqrt{(\mathbf{s}_{i1}^T\mathbf{A}_i)^2-\mathbf{A}_i^{T\,i}\mathbf{A}_i+l^2} \qquad (11)$$

It can be observed that there exist two solutions for each actuated variable in (11), hence there are totally eight possible solutions for a given end-effector position. The two solutions are mirroring about one plane, which are selected due to the assembling manner of the STPM. In this paper, to enhance the stiffness of the manipulator, the sign "±" in (11) should be "+", hence yield one and only solution of the inverse kinematic problem.

3.3 The Direct Kinematics

Given a set of actuated inputs, the position of the end-effector can be solved by the direct kinematic analysis.

According to these given and unknown parameters, rearranging the items of (7) as

$$\mathbf{p}-\mathbf{B}_i=l\mathbf{s}_{i3} \qquad (12)$$

where $\mathbf{B}_i=\mathbf{a}_i-\mathbf{b}_i+d_i\mathbf{s}_{i1}+l_1\mathbf{s}_{i2}$.

Taking dot-multiplying (12) with itself, eliminating unknown $\mathbf{s}_{i3}$ from (12), and considering (8), yields

$$(p_x-ec_i)^2+(p_y-es_i)^2+(p_z-d_i)^2=l^2 \qquad (13)$$

where $e=a\text{-}b\text{-}l_1$.

Writing (13) for each limb (i=1,2,3), we can obtain an algebraic system of three second-degree equations in the unknowns p_x, p_y and p_z.

Subtracting (13) for i=1 and 2 from (13) for i=3 respectively, yields

$$p_x=k_1p_z+k_{01} \qquad (14)$$

$$p_y = k_2 p_z + k_{02} \tag{15}$$

where $k_{01} = (d_1^2 - d_3^2)/4e$, $k_{02} = (2d_2^2 - d_1^2 - d_3^2)/4e$, $k_1 = (d_3 - d_1)/2e$, $k_2 = (d_1 - 2d_2 + d_3)/2e$.

Substituting (14) and (15) into (13) for i=1, expanding and rearranging the items, a quadratic with single unknown be obtained

$$Lp_z^2 + Mp_z + N = 0 \tag{16}$$

where $L = k_1^2 + k_1^2 + 1$, $M = 2(k_1 k_{01} + k_2 k_{02} - k_1 e - d_1)$, $N = (k_{01} - e)^2 + k_{02}^2 + d_1^2 - l^2$.

To obtained p_z by means of solving the quadratic (16)

$$p_z = \frac{-M \pm \sqrt{M^2 - 4LN}}{2L} \tag{17}$$

Once p_z is found, p_x and p_y can be solved by using (14) and (15) in sequence, the direct problem is solved. It can be seen that the direct kinematic problem of the STPM has two possible solutions. Referring to the configuration as shown in Fig. 3, the sign "±" in (17) should be "-".

Clearly, both the inverse and direct kinematic problems of the STPM have only one solution in analytical form, which is advantaged for trajectory generating and real-time control of the STPM.

Table.1 Architectural parameters of the STPM

Parameters	Value (*mm*)	Parameters (for i=1,2,3)	Value (*radian*)
A	300	$\theta_{i,2}$, $\theta_{i,3}$	$0 \sim \pi/2$
B	50	θ_{iP4} (R-pairs of P_A joint)	$-\pi/4 \sim \pi/4$
L	300	φ_i	$(i\text{-}1)\pi/2$
l_1	30	-	-
d_{imax}	d_{imin} +600	-	-

4 A Case Study and Workspace

It is well known that the PMs have relatively small workspaces, which compared with their serial counterparts. Thus the workspace of a PM is one of the most important aspects to reflect its performance, and it is necessary to analyze the shape and volume of the workspace for enhancing applications of PMs [10,11,15]. The reachable workspace boundary and volume of the 3-PRP$_A$R STPM are determined by a numerical method, in terms of the inverse kinematic solutions in the previous section.

The architectural parameters of the STPM are described in Table 1. Assume that **p**=[p_x, p_y, p_z] =[0,0,0] is the initial configuration of the STPM. Taking (11), we can get d_{imin}=203.96*mm*. Its reachable workspace boundary and volume are calculated by a developed MATLAB program and

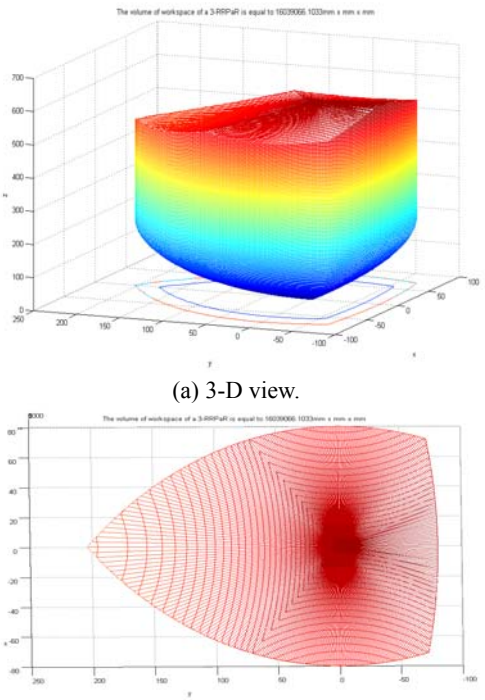

(a) 3-D view.

(b) Top view.

Fig. 4 The workspace of the STPM

illustrated in Fig. 4. The workspace volume of the STPM can be obtained as 16039066.1033mm^3.

From this case study, it is observed that the reachable workspace of the STPM is approximately a regular shape from overlook, and the cross sections on Cartesian frame *x-y* plane like an electric iron. The reachable workspace can be divided into the former and the latter parts, from top views. The former part has a small proportion of entire workspace and it is a triangular approximately. The major latter part of the workspace has regular shape as a square. On the other hand, the STPM with P actuators as shown in Fig. 2 has the workspace advantage along *z* axis and its reachable workspace is a cubical approximately, if the actuation range [d_{imin}, d_{imax}] is long enough.

5 Jacobian Matrix

The Jacobian matrix is defined as the matrix that maps the relationship between the end-effector velocity and actuated P joints rates. The Eq. (7) can be differentiated with respect to time to obtain the velocity equations of i-th limb, which leads to

$$\begin{aligned}&(p_x - ec_i)\dot{p}_x + (p_y - es_i)\dot{p}_y + (p_z - d_i)\dot{p}_z \\ &= (p_z - d_i)\dot{d}_i\end{aligned} \tag{18}$$

Rearranging Equations (18) in a matrix form

$$J^{dir}\begin{bmatrix}\dot{p}_x & \dot{p}_y & \dot{p}_z\end{bmatrix}^T = J^{inv}\begin{bmatrix}\dot{d}_1 & \dot{d}_2 & \dot{d}_3\end{bmatrix}^T \tag{19}$$

where, $\dot{\mathbf{p}} = [\dot{p}_x \quad \dot{p}_y \quad \dot{p}_z]^T$ is the output velocity vector of the end-effector, $\dot{\mathbf{d}} = [\dot{d}_1 \quad \dot{d}_2 \quad \dot{d}_3]^T$ denotes input actuated prismatic joint rates, and J^{dir} and J^{inv} are the direct and the inverse Jacobian matrices respectively.

$$J^{dir} = \begin{bmatrix} p_x - e & p_y & p_z - d_1 \\ p_x & p_y - e & p_z - d_2 \\ p_x + e & p_y & p_z - d_3 \end{bmatrix} \qquad (20)$$

$$J^{inv} = diag[p_z - d_1 \quad p_z - d_2 \quad p_z - d_3]$$

When the STPM is away from singularity, the following velocity equation can be derived from (19)

$$[\dot{d}_1 \quad \dot{d}_2 \quad \dot{d}_3]^T = J[\dot{p}_x \quad \dot{p}_y \quad \dot{p}_z]^T \qquad (21)$$

where

$$J = J^{-inv} J^{dir} \qquad (22)$$

is the 3×3 Jacobian matrix of the STPM, which relates the output velocities to the actuated joint rates.

6 Dexterity

The accuracy of the control of the PMs depends on the condition number of the Jacobian matrix [17]. The dexterity is defined as the reciprocal condition number. This condition value is to be kept as small as possible, the smallest value that can be attained being unity, which is a value associated with isotropic matrices. The condition number of the STPM is defined as that of its Jacobi, namely

$$k = \|J\| \cdot \|J^{-1}\| \qquad (23)$$

where $\|\bullet\|$ denotes the Euclidean norm.

Since the Jacobian matrix depends on the configuration. The k can also be used to evaluate the distance to the singularity. The k=1 means that the STPM is in its isotropy configuration, the larger k that can be close to singular configuration.

Taking the architectural parameters in previous section, the distributions of condition number of the STPM in x-y plane (while p_z=300mm), x-z plane (while p_y=0mm), and x-y plane (while p_x=0mm) are shown in Fig. 5. From Fig. 5(a), it is seen that condition number is minimal when the end-effector lies along the z axis, and increases in case of the STPM approaching to its workspace boundary. It can be observed from Fig. 5(b) and 5(c) that in x-z and y-z planes, the condition number is minimal when the center point of the end-effector lies in the z axis, there are invariant along the z axis, and increases when the end-effector is away from the z axis.

Entirely, the maximal value of the condition number is 2.1, minimal value is 1.3, and the minimal value distributes on the z axis. Thus we concluded that the dexterity of the STPM decreases from the z axis to the workspace boundary, its maximal dexterity distributes on the z axis, and each configuration inside of the workspace is far from the singularity.

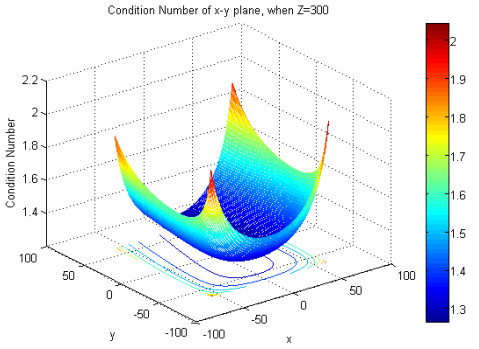

(a) The x-y plane, while z=300.

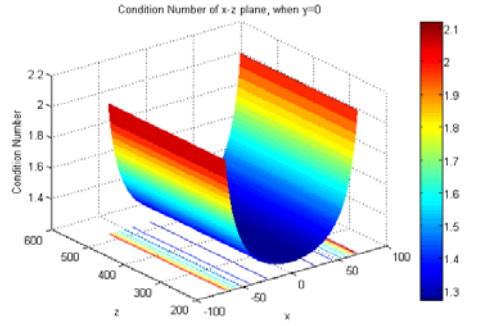

(b) The x-z plane, while y=0.

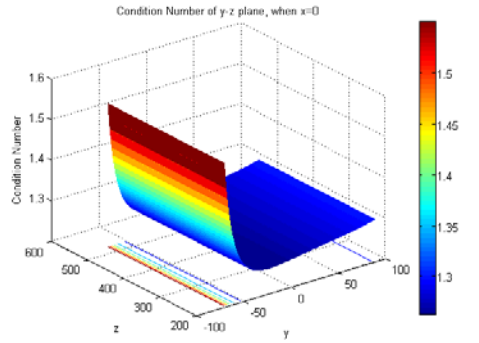

(c) The y-z plane, while x=0.

Fig. 5 The Condition Number of the STPM

7 Conclusion

In this paper, a new STPM with mounted-base actuated P joint is proposed, which has three PRP_AR limbs. After a short of description of the STPM, the angular velocity of the end-effector is analyzed. Both the inverse and the direct kinematic problems were solved in analytical form. The workspace

boundary and volume of the STPM are determined by numerical method in a case. The Jacobian matrix has been derived, and the distribution of the condition number on the different planes is given. We can concludes that:

(1) Although the inverse kinematic problem produces two possible solutions for each limb and the direct kinematics have two possible solutions theoretically, but they have only one solution due to the assembling manner of the STPM, which is advantaged for real-time control of the STPM.

(2) The reachable workspace of the STPM is regular, approximately as a cuboid, and has an advantage along *z* axis.

(3) The distribution of the condition number of Jacobian matrix on the *x-y* plane, *x-z* plane, and *y-z* plane are generated by a numerical approach. The condition number value of the STPM is increased from the *z* axis to the workspace boundary. Its minimal and maximal values are 1.3 and 2.1 respectively, and the minimal value distributes on the *z* axis. Therefore, each configuration inside of the workspace is far from the singularity.

As for the future works of this new STPM, we propose: (*a*) further investigations into kinetostatics performance index, optimal design, (*b*) the dynamic modeling, control issues, and (*c*) develop a prototype of this STPM for polishing application.

Acknowledgment

The authors appreciate the fund support from National Natural Science Foundation of China (No. 50575208). and Zhejiang Province Natural Science Foundation (No. M503099).

References:

[1] Clavel R., Device for the movement and positioning of an element in space, *United States Patent*, No. 4,976,582, 1990.

[2] Hervé J. M., and Sparacino F., Structural synthesis of parallel robots generating spatial translation, *IEEE Int. Conf. on Advanced Robotics*, Pisa, Italy, 1991, pp. 808-813.

[3] Tsai L. W., and Joshi S., Kinematics and optimization of a spatial 3-UPU parallel manipulator, *ASME J. Mech. Design*, Vol.122, No.4, 2000, pp.439-446.

[4] Frisoli A. et al., Synthesis by screw algebra of translating in-parallel actuated mechanisms, *Advances in Robot Kinematics, eds. J. Lenarčič, and M. M. Stanišić, Kluwer Academic*, Dordrecht, 2000, pp. 433-440.

[5] Carricato M., and Parenti-Castelli V.. A family of 3-DoF translational parallel manipulators, *ASME Design Eng. Tech. Conf.*, Pittsburgh, PA, 2001, DAC-21035.

[6] Tsai L. W., Kinematics of a three-DoF platform with three extensible legs, *Recent Advances in Robot Kinematics, eds. J. Lenarčič and V. Parenti-Castelli, Kluwer Academic*, Dordrecht 1996, pp. 401-410.

[7] Di Gregorio R., and Parenti-Castelli V., Mobility analysis of the 3-UPU parallel mechanism assembled for a pure translational motion, *IEEE/ASME Int. Conf. on Advanced Intelligent Mechatronics*, Atlanta, GA, 1999, pp. 520-525.

[8] Shen H., et al., Structure and displacement analysis of a novel three-translation parallel mechanism, *Mech. Mach. Theory*, Vol.40, No.10, 2005, pp.1181-1194.

[9] Sparacino F., and Hervé J. M., Synthesis of parallel manipulators using Lie-Groups — Y-Satar and H-Robot, *IEEE/Tsukuba Int. Workshop on Advanced Robotics*, Tsukuba, Japan, 1993, pp. 75-80.

[10] Tsai L. W., Walsh G. C., and Stamper R. E., Kinematics of a novel three DoF translational platform, *IEEE Int. Conf. on Robotics and Automation*, Minneapolis, USA, 1996, pp. 3446-3451

[11] Wenger P., and Chablat D., Kinematic analysis of a new parallel machine tool: the Orthoglide, *Advances in robot kinematics, eds. J. Lenarčič and M.M. Stanišić, Kluwer Academic*, Dordrecht, 2000, pp. 305-314

[12] Zhao T. S., and Huang Z., A novel three-DoF translational platform mechanism and its kinematics, *ASME Design Eng. Tech. Conf.*, Baltimore, MD, MECH-14101. 2000.

[13] Jin Q., and Yang T. L., Position analysis for a class of novel 3-DoF translational parallel robot mechanisms, *ASME Design Eng. Tech. Conf.*, Pittsburgh, PA, DAC-21151. 2001.

[14] Massimo C., and Matteo T., Kinematic analysis of a novel translational platform, *ASME J. Mech. Design*, Vol.125, No.6, 2003, pp.308-315.

[15] Li Y., and Xu Q., Kinematic analysis and design of a new 3-DOF translational manipulator, *ASME J. Mech. Design*, Vol.126, No.7, 2006, pp.729-737.

[16] Zlatanov, D., et al., Constraint singularities of parallel mechanisms, *IEEE Int. Conf. on Robotics and Automation*, Washington, DC, 2002, pp. 496-502.

[17] Gosselin C. M., and Angeles J., A global performance index for the kinematic optimization of robotic manipulators, *ASME, J. Mech. Design*, Vol.113, No.9, 1991, pp.220-226.